DD

FEDERAL SCIENCE CENTRE

INSTITUTE FOR HIGH ENERGY PHYSICS

IHEP 94-103

S.Denisov, A.Dushkin, N.Fedjakin, Yu.Gilitsky,
V.Kochetkov, V.Mikhailin, Yu.Mikhailov,
V.Onuchin, I.Shein, A.Soldatov,
A.Spiridonov, V.Sytnik

HADRON GAS IONIZATION CALORIMETERS WITH STEEL AND LEAD ABSORBERS

Submitted to Nuclear Instruments and Methods

Protvino 1994

UDK 539.1.074.55

M-24

Abstract

Denisov S., Dushkin A., Fedjakin N. et al. Hadron Gas Ionization Calorimeters with Steel and Lead Absorbers: IHEP Preprint 94-103. – Protvino, 1994. – p. 15, figs. 16, tables 2, refs.: 6.

The characteristics of two gas ionization calorimeters with planar electrode geometry have been studied in hadron and electron beams of the 70 GeV IHEP accelerator. Steel and lead absorbers with thickness of 11.8 and 12.9 g/cm^2 were used. The calorimeters were filled with $90\%Ar + 10\%CF_4$ gas mixture at a pressure up to 25 atm. The dependencies of calorimeter response and energy resolution on gas pressure , absorber thickness, gate width and delay, hadron energy and thickness of the entrance window are presented. The data on position resolution and electron-to-hadron signal ratio are discussed.

Аннотация

Денисов С.П. и др. Адронные газовые ионизационные калориметры со стальными и свинцовыми поглотителями: Препринт ИФВЭ 94-103. – Протвино, 1994. – 15с., 16 рис., 2 табл., библиогр.: 6.

Характеристики двух газовых ионизационных калориметров с плоскопараллельной геометрией электродов исследованы в пучках адронов и электронов. Были использованы стальные и свинцовые поглотители с толщинами 11.8 и 12.9 г/см^2. Представлены зависимости отклика и энергетического разрешения калориметров от толщины слоя поглотителя, ширины ворот и задержки, энергии адронов и толщины входного окна детектора. Обсуждаются координатное разрешение и отношение величин сигналов от электронов и адронов.

Introduction

The first study of a gas ionization calorimeter in hadron beams performed at the 70 GeV IHEP accelerator demonstrated that this type of calorimetry had good energy and time resolution, high uniformity and stability, simple calibration, high radiation resistance, relatively low cost and can play an important role in future experiments in high energy physics [1, 2]. The absorbers of the calorimeter tested were made of uranium. Although uranium is often used in calorimetry it has well known drawbacks which are high cost and radiaoctivity. In 1993-94 we investigated the characteristics of gas ionization calorimeters with steel and lead absorbers. The preliminary results of this study were reported at the 1993 Calorimetry Conference [3]. The results of complete data analysis are presented below.

1. Calorimeters

The calorimeters described have a planar electrode geometry. In comparison with other solutions (spacal, accordion) the planar geometry has the following attractive features:

- any absorber material can be used,
- fine granularity in both longitudinal and transverse directions may be easily achieved,
- very good uniformity.

The two calorimeter structures are shown in fig. 1. Each calorimeter consists of a stack of ionization chambers interleaved with passive absorbers. The transverse size of the absorbers is 58×58 cm^2. The total thickness of the calorimeters is 7.4 λ. Signal electrodes made of 1.5 mm G-10 were placed between the absorbers forming two 4 mm drift gaps. On each side of the electrodes there are 3 vertical signal strips 14 cm wide and 42 cm high.

The stack of absorbers and signal planes are contained in a cylindrical stainless steel vessel designed to operate at up to 40 atm [1, 2]. The vessel has a 2 mm steel window for a beam. It was filled with $90\%Ar + 10\%CF_4$ gas mixture. The HV applied to the signal strips was equal to 180 V/atm, which corresponds to a maximum electron drift velocity of 0.12 mm/ns [4]. So the maximum drift time of electrons was 33 ns.

Signals from each strip were transported to amplifiers [1, 2], using 4 m 50 Ohm cable. The δ-function response of the electronics chain has a 30 ns base width. ADC gate widths of 25, 55, or 145 ns were used in most of the measurements. A part of the measurements were performed with the gate width varied from 19 to 240 ns.

The measured noise level for one channel is $\sigma = 9$ ke (55 ns gate) which is in a good agreement with the calculated value. The dependence of the noise for all 225 channels on the gate width is shown in fig. 2. The value at 55 ns is close to that expected for uncorrelated noise. It means that the contribution of the coherent noise is negligible.

2. Measurements and pulse height spectra

Measurements have been performed using $26 \div 58$ GeV/c negative hadron beams and a 26.6 GeV/c electron beam produced in the internal targets of the 70 GeV IHEP accelerator. The composition of the hadron beams is π^- ($> 96\%$), K and μ ($1 \div 2.5\%$), e and p ($< 1\%$). The hadron contamination of the electron beam is less than 1%. The typical beam momentum spread was 3%.

The studies consisted in measuring the pulse height distributions at different values of the particle momentum, gas pressure, gate width and gate delay. Samples of $3 \cdot 10^3$ to $12 \cdot 10^3$ events were detected for each spectrum. The noise spectrum was measured before and after the data collection for each set of parameters. Twice per day the detector was calibrated.

Events satisfying the following criteria were selected for analysis:

- the shower vertex is between the 3-rd and 10-th electrode,
- the signal in the central strips is twice as large as that in the side strips.

The first criterion allowed one to avoid the corrections connected with the shower energy leakage and muon contamination in the beam [2, 3]. The second criterion was used to reject the events when beam and halo particles passed through the detector simultaneously (typically 1% of events were rejected by this criterion).

A typical pulse height distribution for selected events is shown in fig. 3. This distribution and data presented below were measured at 24 atm gas pressure unless stated otherwise. All the spectra for selected events are well fitted by a Gaussian. There is no indication for any tails on the pulse height distributions due to "Texas towers" or other effects.

3. Average pulse heights

The dependences of the average signal on the gas pressure P, gate width t_g, gate delay t_d, and shower energy E are presented in figs.$4 \div 7$. The following conclusions can be derived from these data:

- 25, 55, and 145 gates contain 45, 70 and 98 % of total ionization signal, respectively (fig. 4b),
- maximum pulse height coresponds to $t_d = 0$ ($t_g = 145$ ns), $t_d = 10$ ns ($t_g = 55$ ns) and $t_d = 20$ ns ($t_g = 25$ ns), (see figs. 5, 6),

- the ratio of hadron signals from steel and lead calorimeters is equal to 1.4 ± 0.1 (fig. 5); the same ratio for electrons is about 1.6 ± 0.1 (fig. 6),
- signal-to-noise ratio depends weakly on the gate width (compare figs. 2 and 4b): this means that the equivalent noise energy is about the same for all values of t_g,
- the detector response is linear (fig. 7).

The data shown in figs. 4, 7 and presented below were measured with $t_d = 0$ ($t_g = 145$ ns) and $t_d = 20$ ns ($t_g = 25, 55$ ns).

4. Energy resolutions

Figs. 8, 9 show energy resolution σ/E vs gate width and gate delay. From these figures it follows that for gate delays chosen the energy resolution depends weakly on the gate width and reaches an optimum value.

Due to the fine longitudinal granularity of the calorimeters it was possible to study the energy dependence of the energy resolution for the different absorber thickness t by summing the signal not only from all planes, but from odd and even planes separately, from each 3-rd plane and so on. The values of σ/E_h for hadrons obtained by this method are well fitted using the formula [5] (see fig. 10)

$$\frac{\sigma}{E} = \frac{A}{E} \bigoplus \left(\frac{B}{\sqrt{E}} + C \right) , \tag{1}$$

where the parameters A and B represent the equivalent noise energy and the stochastic fluctuations of the shower energy deposited in the working gas. The values of A, B, and C are presented in Table 1. The parameter A was estimated using signal and noise pulse height spectra. The constant term C was assumed to be independent of the absorber thickness t. Typical errors on the parameters are 0.03 for B and 0.004 for C.

The stochastic fluctuations are less for the steel calorimeter than for the lead calorimeter; the latter has values of C that are equal to zero within the errors quoted. It is worth mentioning that no corrections were applied to take into account the possible energy leakage in the transverse direction.

The dependence of the stochastic parameter B on the absorber thickness t is well fitted by either of the formulae (see fig. 11)

$$B(t) = b\sqrt{t} \bigoplus c \, , \tag{2}$$

$$B(t) = b'\sqrt{t} + c' \, . \tag{3}$$

Parameters b and c represent the contribution of the sampling and intrinsic fluctuations to the stochastic part of the energy resolution and are listed in Table 2. From Table 2 it follows that for the steel calorimeter the sampling and intrinsic fluctuations give about equal contribution to the parameter B while for the calorimeter with lead absorbers the sampling fluctuations are more important. The data on the t-dependence can be used to estimate the absorber thickness required for the calorimeter with a desired energy resolution.

Fig. 12 demonstrates that the contribution of hadron shower fluctuations to energy resolution depends weakly on the gas pressure up to 5 atm. The same conclusion was reached for a gas calorimeter with uranium absorbers [2].

Table 1. Parameters in formula (1). t_0 is the thickness of one absorber. A and B are measured in GeV and $\sqrt{GeV}$

Absorber	Gate width, ns	Para meter	Absorber thickness				
			t_0	$2t_0$	$3t_0$	$4t_0$	$5t_0$
steel	25	A	6.0	9.0	11.0	12.9	14.4
		B	0.71	0.82	0.98	1.07	1.22
		C	0.025				
	55	A	5.0	7.6	9.5	11.0	12.3
		B	0.70	0.85	0.94	1.07	1.18
		C	0.045				
	145	A	5.0	7.5	9.2	10.6	11.7
		B	0.77	0.88	1.00	1.18	1.27
		C	0.044				
lead	25	A	7.1	10.2	12.5	14.5	16.3
		B	0.84	1.12	1.32	1.49	1.67
		C	0.001				
	55	A	6.6	9.5	11.7	13.6	15.3
		B	0.82	1.08	1.30	1.42	1.62
		C	0.002				
	145	A	6.1	8.8	10.6	12.3	13.8
		B	0.92	1.16	1.37	1.50	1.70
		C	0.003				

Table 2. Parameters in formulae (2),(3) for units B in $\sqrt{GeV}$ and t in units of t_0

Absorber	Para meter	Gate width, ns		
		25	55	145
steel	b	0.49	0.47	0.50
	b'	0.40	0.38	0.41
	c	0.50	0.51	0.56
	c'	0.29	0.31	0.33
lead	b	0.72	0.69	0.71
	b'	0.66	0.64	0.62
	c	0.44	0.45	0.59
	c'	0.17	0.18	0.29

In the runs with the electron beam signals from 35 (15) forward layers of the steel (lead) calorimeter were detected. The total thickness of these layers is about 30 r.l. Direct calculations taking into account the momentum spread of this beam, and the method of interleaved calorimeters were used to estimate the energy resolution for EM showers. The last technique permits the cancellation of all the systematic effects and uncertainties including the momentum spread of the beam. Both approaches have given the same result. For t_g=55 ns (E_e in GeV):

$$\frac{\sigma}{E_e} = \frac{2.8}{E_e} \bigoplus \frac{0.25}{\sqrt{E_e}} \qquad (steel \quad absorbers)\,,$$

$$\frac{\sigma}{E_e} = \frac{2.6}{E_e} \bigoplus \frac{0.28}{\sqrt{E_e}} \qquad (lead \quad absorbers)\,.$$

Both the equivalent noise energy and the stochastic term are almost independent of t_g. Results of a MC simulation are in a good agreement with the experimental data. They show that the constant term in the energy resolution for electrons is less than 1% for both steel and lead calorimeters.

For the gas ionization calorimeter operating at high pressure it is important to investigate the dependence of its characteristics on the thickness of the entrance window. This was done by neglecting the signals from the front layers. The results presented in fig. 13 show that the passive material in front of the calorimeter has negligible influence on its response and energy resolution up to 2 r.l. for electrons and up to 0.5 λ for hadrons. The degradation of the average pulse height and the energy resolution above these values can not be explained by reducing the total calorimeter thickness (see fig. 15 in [2]) and is due to increasing the amount of passive material.

5. e/h ratio and position resolution

The ratio of calorimeter response to electrons and hadrons (e/h ratio) depends on the gate width and delay (fig. 14). This behaviour can be explained by different shapes of hadron and electron signals: an electron signal is shorter than a hadron one. Usually it is important to keep the e/h ratio as close to unity as possible. Fig. 14b shows that this can be done for the lead calorimeter by using the short gate width ($\sim$ 25 ns) and $t_d \approx 30$ ns, while at the optimum value of $t_d \approx 20$ ns $e/h \approx 1.1$. In the case of the steel calorimeter e/h is higher: 1.15 at $t_d = 30$ ns and 1.2 at $t_d = 20$ ns. It is well known that the constant term in the energy resolution depends on the e/h ratio: the closer e/h is to 1 the smaller the constant term is. So the results on e/h ratio are in a qualitative agreement with values of the parameter C in formula (1).

The distribution of the difference $\Delta = x_p - x_s$, where x_p and x_s are the horizontal coordinates of incoming hadron and shower axis is presented in fig. 15. The trajectory of incoming particle was defined by a small (1 $\times$ 1 cm^2) trigger counter placed in front of the calorimeter. The coordinate of the shower axis was estimated by the center of gravity method. Δ-distributions were fitted to a Gaussian. The parameters σ_x of the Gaussian distributions obtained from the fit were as a rule in a good agreement with the RMS values of the Δ-distributions. The dependence of the position resolution σ_x on hadron energy is shown in fig. 16. The experimental data were fitted to the formula which

takes into account both the shower fluctuations and electronic noise. Position resolutions measured with a steel/stintillator sandwich calorimeter [6] of about the same transverse granularity are shown in the fig. 16 for comparison.

Conclusion

The characteristics of two fine grain gas ionization calorimeters (with steel and lead absorbers) have been studied in hadron and electron beams. All the pulse height spectra measured have a pure gaussian shape. The energy dependence of the energy resolution for hadron showers are well fitted to the standard formula containing stochastic, constant and noise terms. Stochastic term B depends weakly on the gas pressure up to 5 atm and is equal to $0.7 \div 0.8$ for the steel calorimeter and $0.8 \div 0.9$ for the lead one. With thinner absorbers one can reach a B value of ~ 0.5. It is shown that sampling and intrinsic fluctuations give about equal contribution to the parameter B of the steel calorimeter, while for the lead one the sampling fluctuations are more important. The constant term C is about 4% for the steel absorbers. For the lead calorimeter $C = 0$ within the errors. The e/h ratio depends on the ADC gate width and delay. This can be explained by different shapes of hadron and electron signals. The e/h of $1.15 \div 1.20$ was obtained for the steel calorimeter. For the lead calorimeter one can reach $e/h = 1$ using a short gate width and large gate delay.

A detailed study of the characteristics of the gas ionization calorimeters with plain electrode geometry shows that they possess good energy, time and position resolutions at rather moderate gas pressures, and that the e/h ratio can be close to unity. Due to high intrinsic radiation resistance this type of calorimetry is especially promising for the forward calorimetry in high luminosity experiments.

Acknowledgements

We would like to thank C. Fabjan and B. Williams for reading the manuscript and giving useful comments.

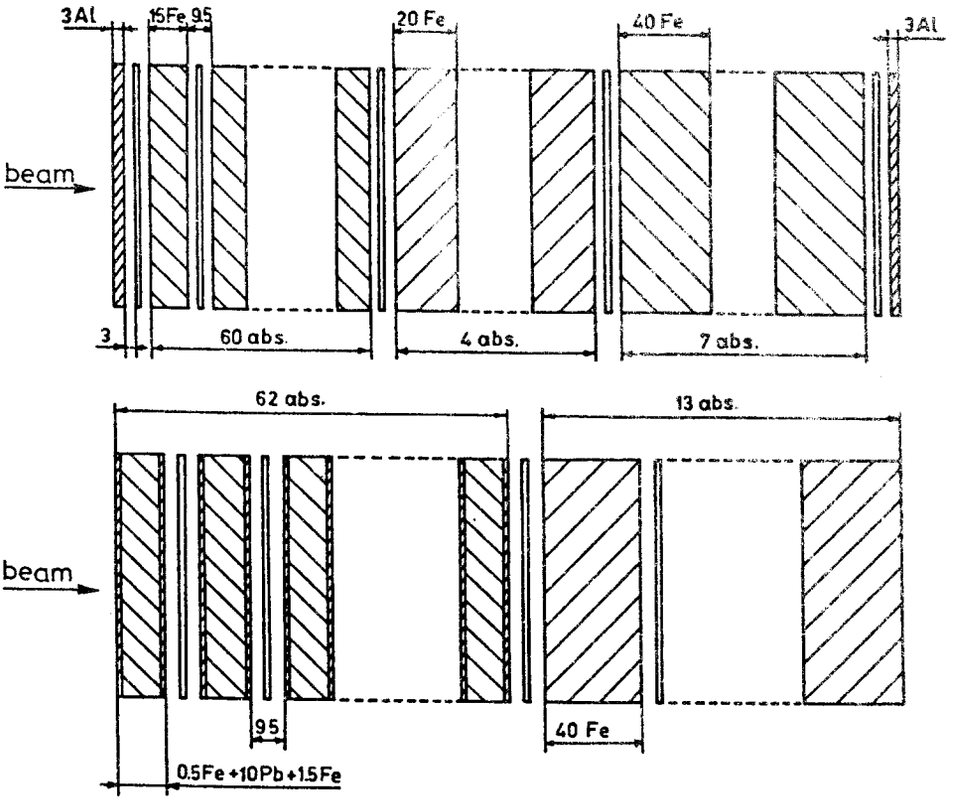

Fig. 1. The two calorimeter structures. Dimensions are in *mm*.

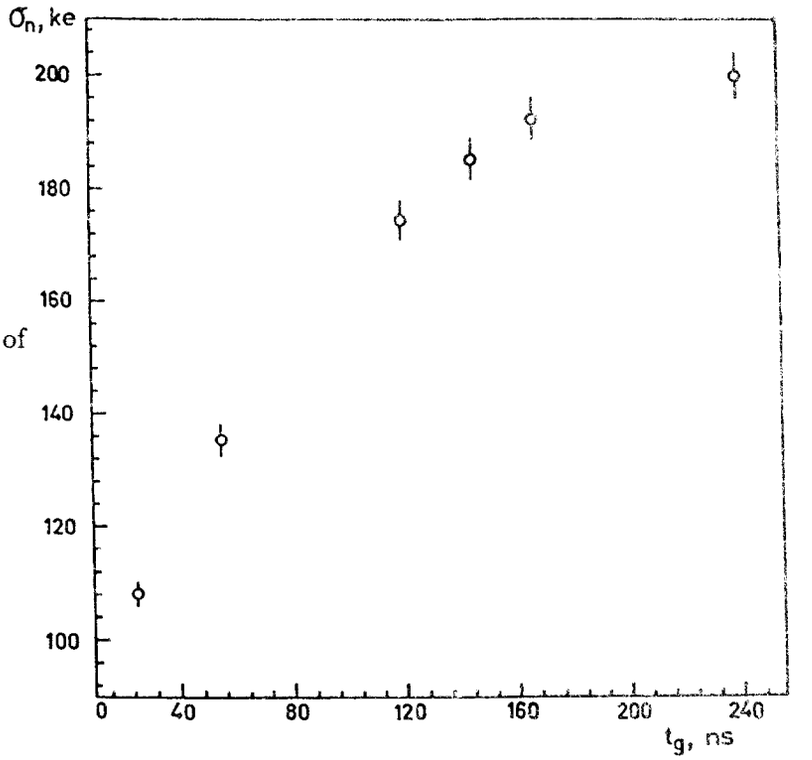

Fig. 2. Noise level as function of the ADC gate width.

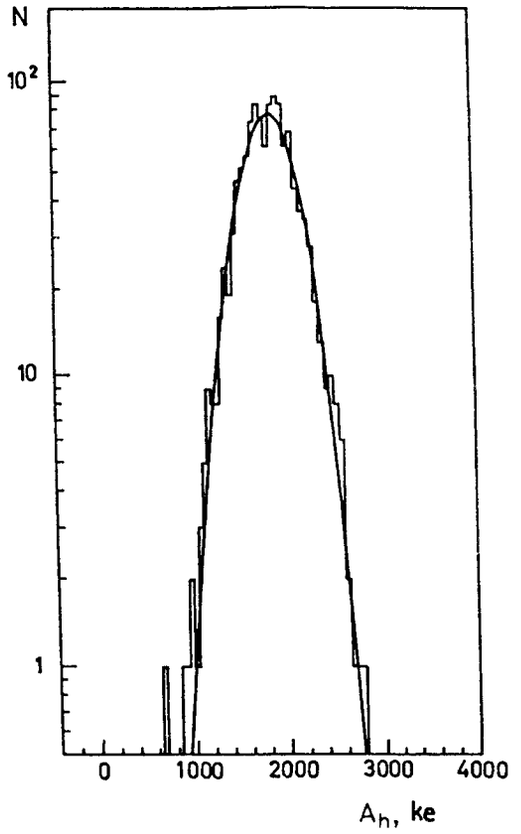

Fig. 3. Pulse height spectrum measured with steel calorimeter in 58 GeV hadron beam (gate width $t_g = 55\ ns$, gate delay $t_d = 20\ ns$).

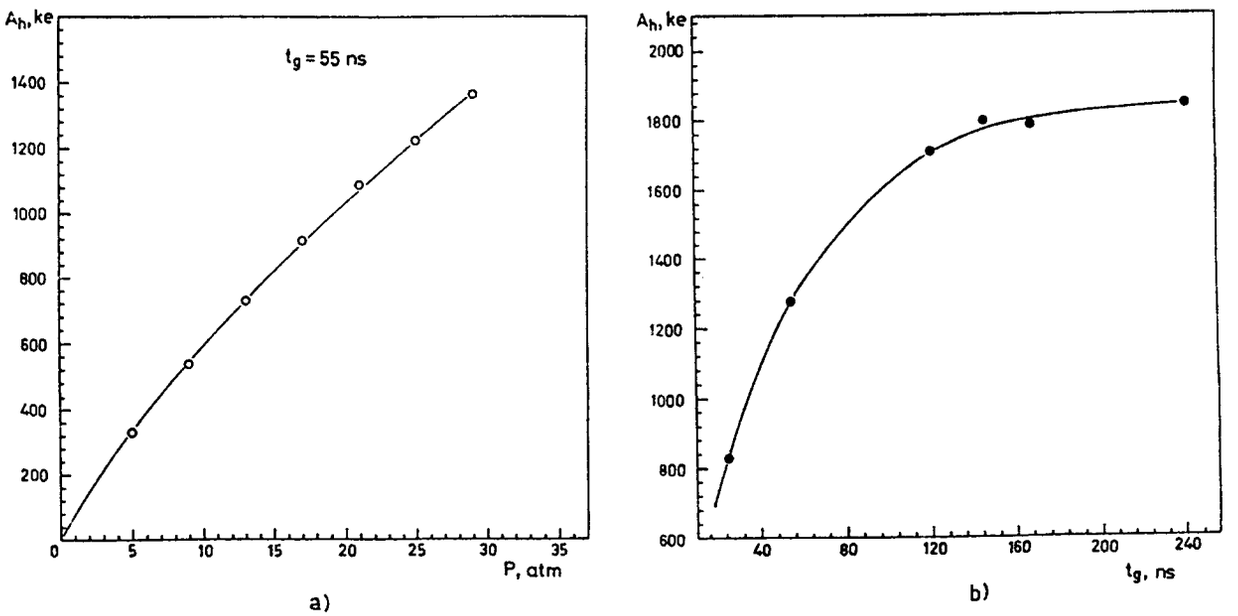

Fig. 4. The dependence of average signal of 58 GeV hadron shower on the (a) gas pressure and (b) gate width measured with lead calorimeter. The curves are drawn by hand.

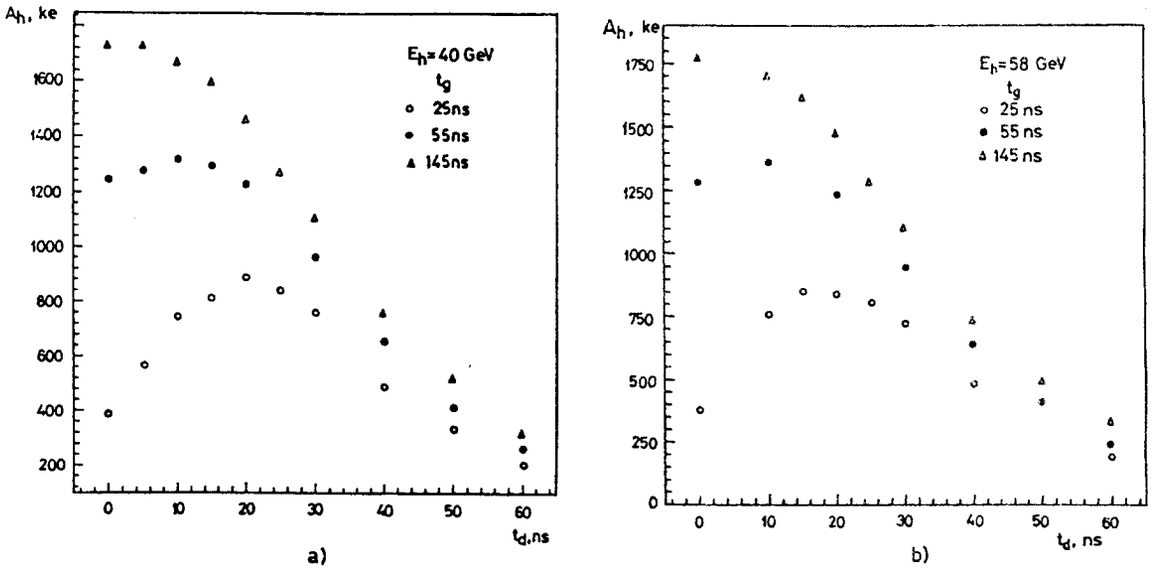

Fig. 5. The dependence of the average hadron signal on the gate delay for (a) steel and (b) lead calorimeters.

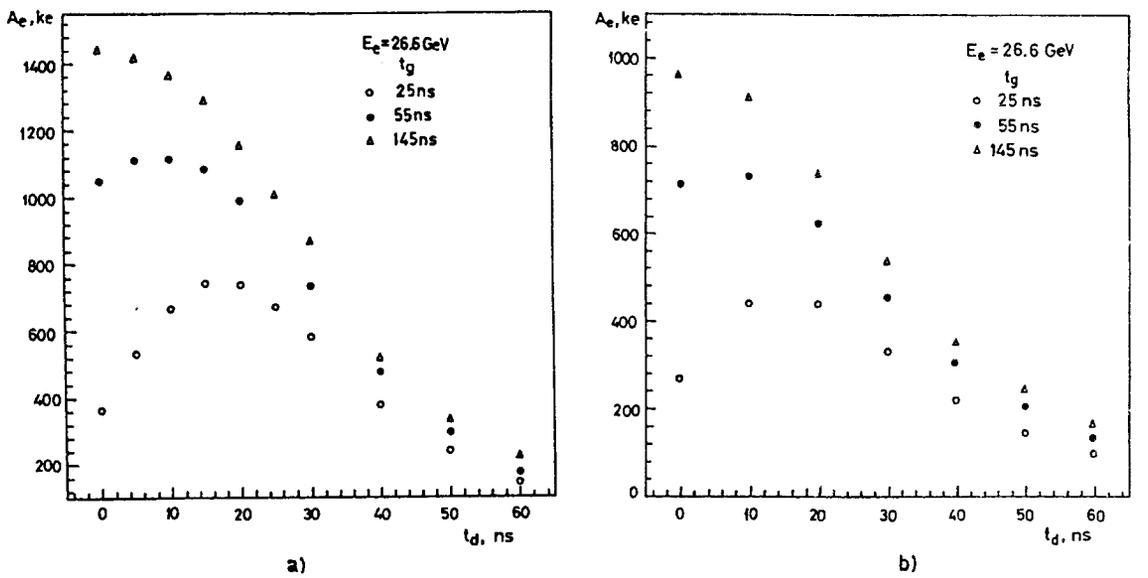

Fig. 6. The dependence of the average electron signal on the gate delay for (a) steel and (b) lead calorimeters.

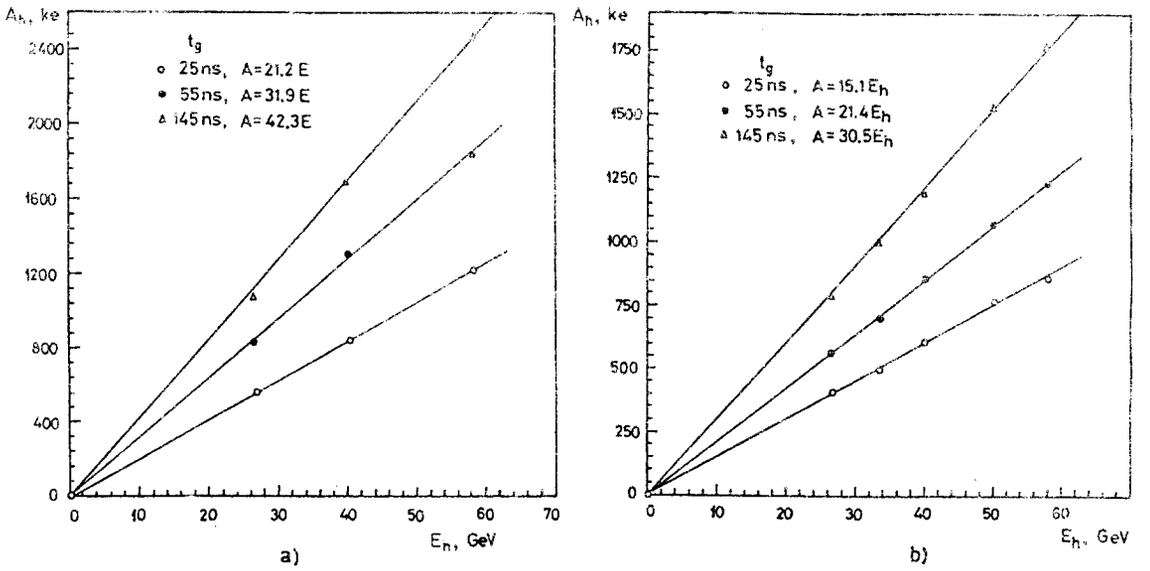

Fig. 7. Energy dependence of the average pulse height for (a) steel and (b) lead calorimeters.

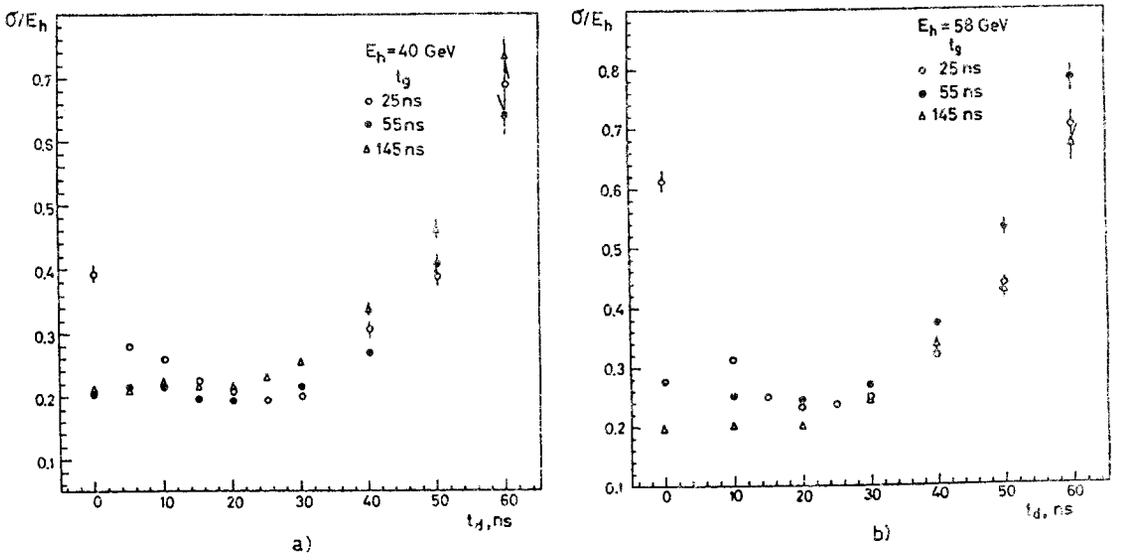

Fig. 8. Hadron energy resolution vs gate delay for (a) steel and (b) lead calorimeters.

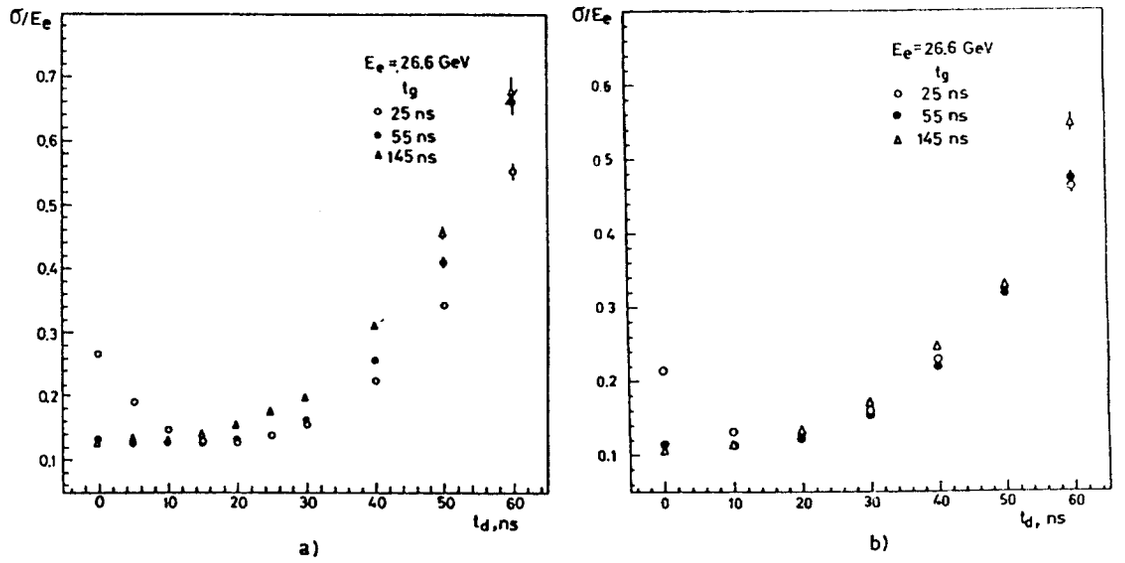

Fig. 9. *EM* energy resolution vs gate delay for (*a*) steel and (*b*) lead calorimeters.

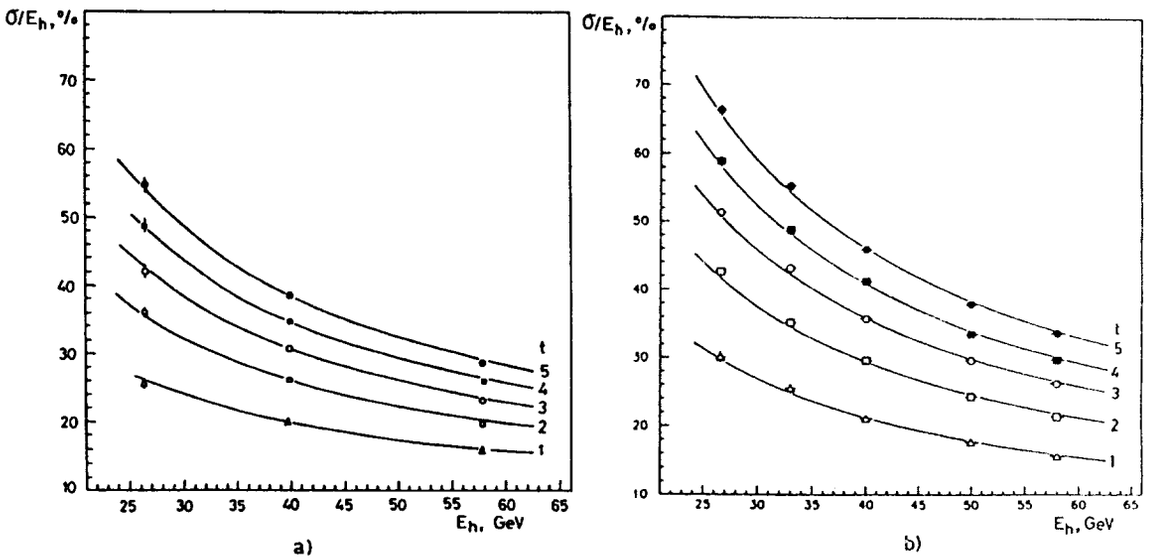

Fig. 10. Energy resolution vs hadron beam energy for (*a*) steel and (*b*) lead calorimeters (t_g = 55 *ns*). Curves represent the eq.(1). Figures near the curves show the absorber thickness measured in the units of $t_0 \approx 0.08\ \lambda$, where t_0 is the thickness of one absorber.

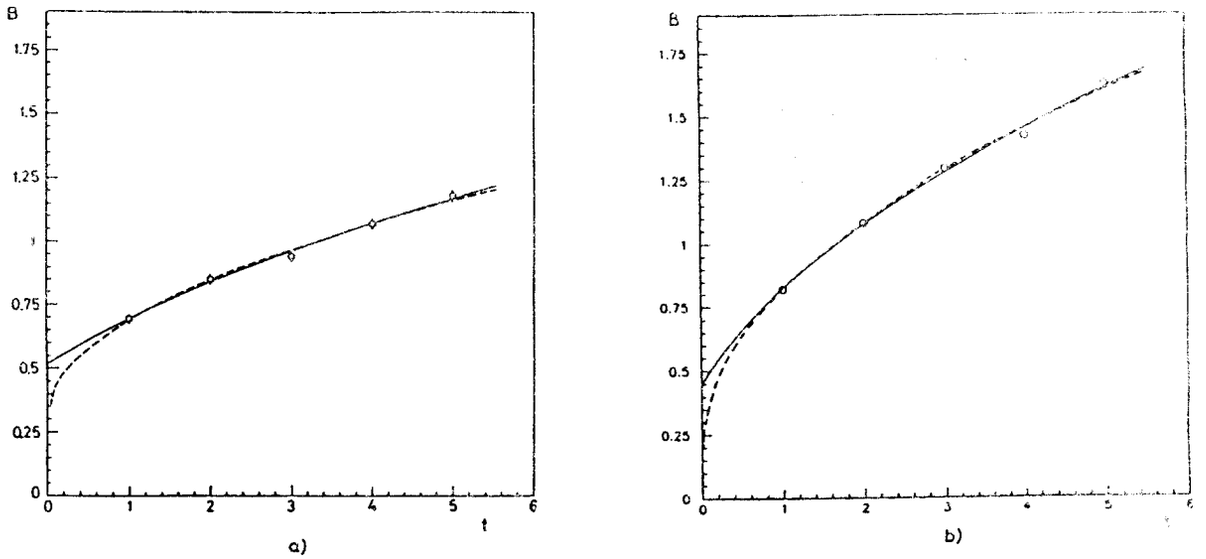

Fig. 11. Stochastic parameter B as a function of absorber thickness t for (a) steel and (b) lead calorimeters ($t_g = 55\ ns$). t is measured in the units of t_0, where t_0 is the thickness of one absorber. The solid and dotted lines represent the eq.(2) and eq.(3) respectively.

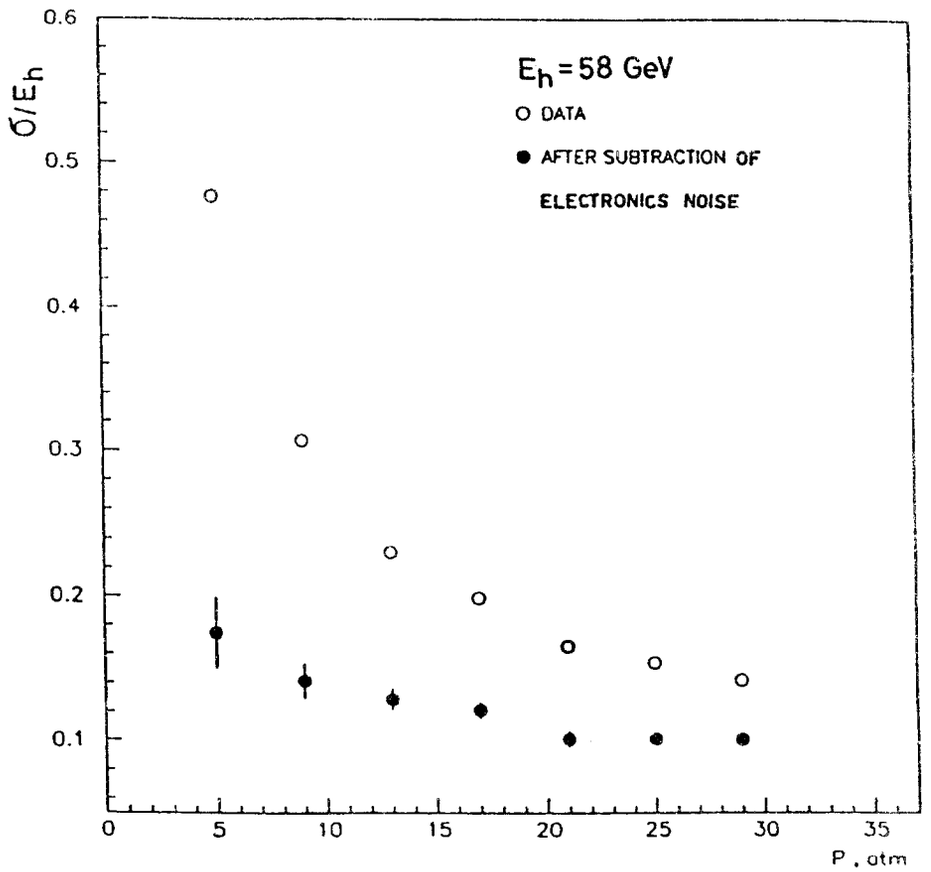

Fig. 12. Energy resolution of the lead calorimeter vs gas pressure ($t_g = 55\ ns$).

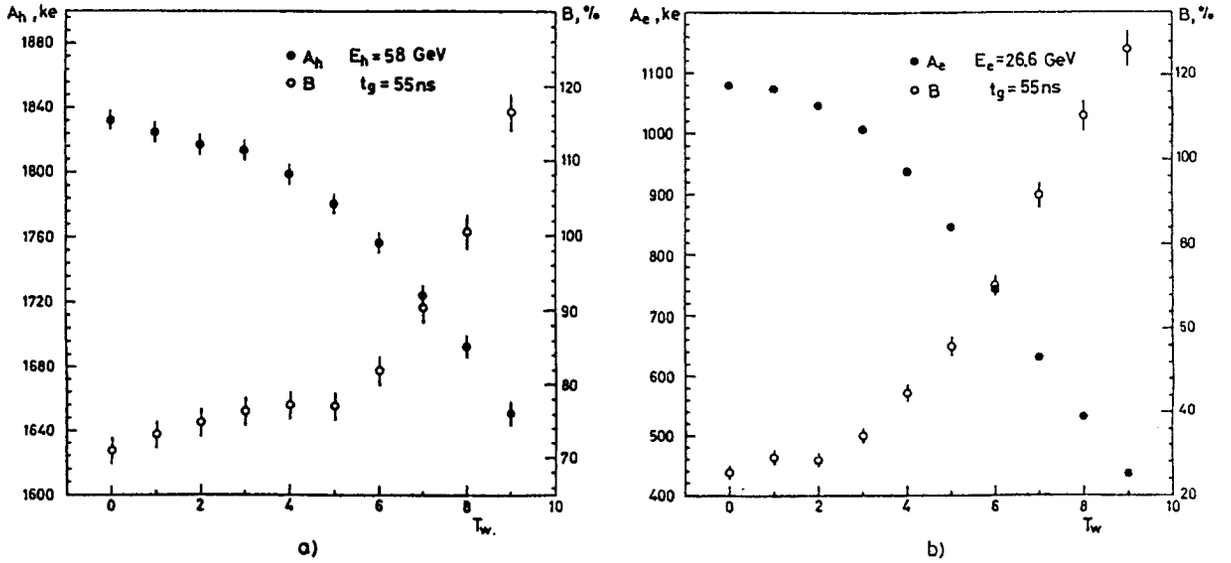

Fig. 13. Stochastic parameter and response for (a) hadron and (b) EM showers vs thickness of passive material in front of the steel calorimeter ($t_g = 55\ ns$). T_W is measured in the units of absorber thickness, t_0.

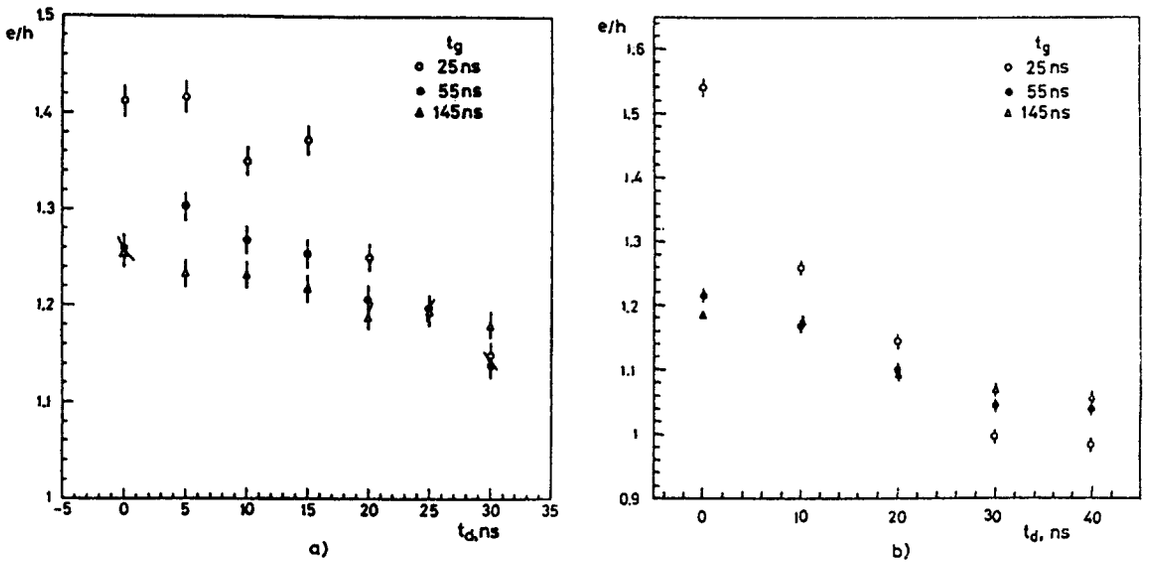

Fig. 14. e/h ratio vs gate delay for (a) steel and (b) lead calorimeters.

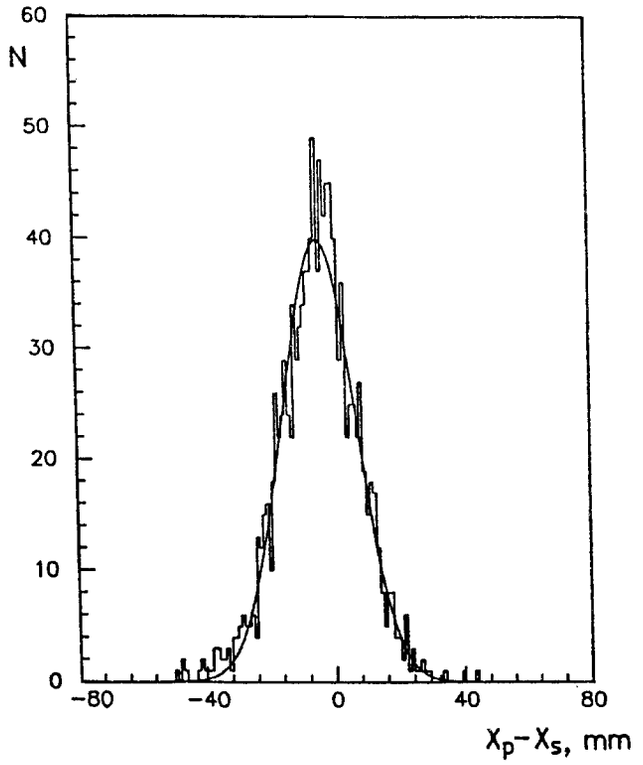

Fig. 15. Distribution of the difference between x-coordinates of the incoming hadron and the shower axis.

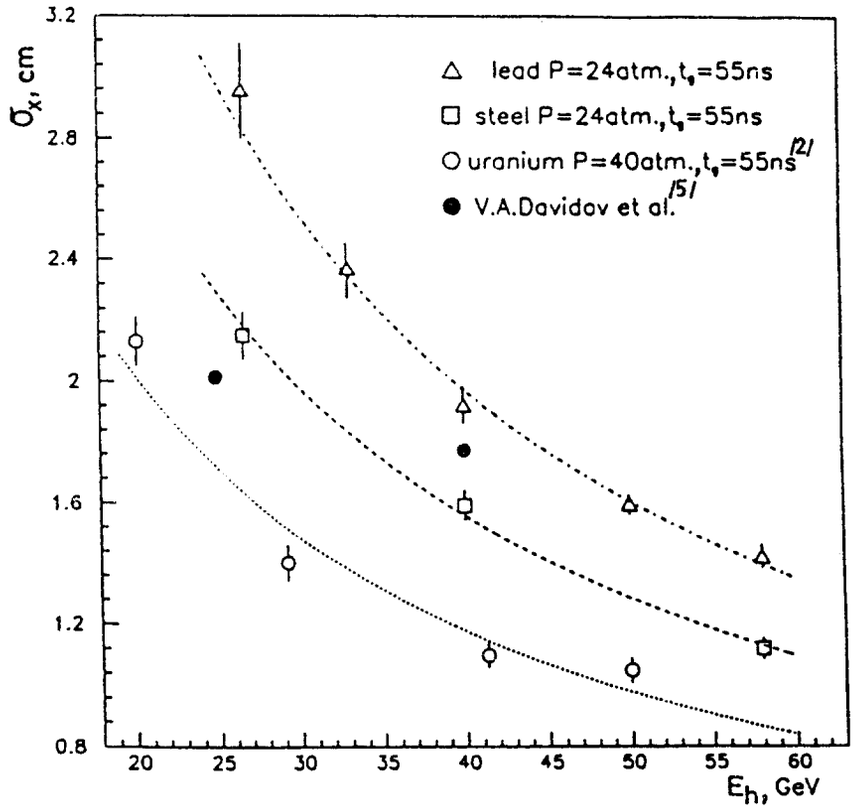

Fig. 16. Position resolution *vs* hadron energy.

References

[1] Yu.V.Gilitsky et al., Pribori i Technika Experimenta, N5, 1993, 34-43.

[2] S.P. Denisov et al., Nucl.Instr.and Meth. A335(1993)106-112.

[3] S.P. Denisov et al., Proceedings of the IV International Conference on Calorimetry, Elba, 1993.

[4] A.Peisert, F. Sauli, CERN Preprint 84-08, Geneva, 1984.

[5] R. Wigmans , Nucl. Instr. and Meth. A259 (1987) 389.

[6] V.A.Davidov et al., Nucl.Instr.and Meth., 174 (1980) 369-377.

Received September 19, 1994.

С.П.Денисов и др.
Адронные газовые ионизационные калориметры со стальными и свинцовыми поглотителями.

Оригинал-макет подготовлен с помощью системы LaTeX.
Редактор Е.Н.Горина.

Подписано к печати 21.09.1994 г. Формат 60 × 84/8.
Офсетная печать. Печ.л. 2,0. Уч.-изд.л. 1,54. Тираж 240. Заказ 53.
Индекс 3649. ЛР №020498 06.04.1992.

Институт физики высоких энергий, 142284, Протвино Московской обл.

Индекс 3649

П Р Е П Р И Н Т 94-103, И Ф В Э, 1994